

Ionic Dissociation Effects in Light Emitting Electrochemical Cells

NICOLETA DOBRE¹, FLORENTINA GOLGOVICI¹, MIHAI BUDA^{1*}

University Politehnica of Bucharest, Faculty of Applied Chemistry and Materials Science, 132 Calea Grivitei, 010737, Bucharest, Romania

The paper describes theoretically the ionic dissociation equilibrium which takes place in operating light-emitting electrochemical cells (LECs), based on a previously developed model. The model can be useful for understanding the behaviour of LECs: it is proposed that the ionic equilibrium may be related to the amount of residual solvent which is present in the film, both simulations and experiment showing that a decrease in the concentration of residual solvent leads to much longer response-times and lower currents. The slow response times may thus be due to two factors: very low dissociation equilibrium constant and very slow ion movement.

Keywords: light emitting electrochemical cells, organic light emitting devices, computational chemistry, molecular electronics

Light-emitting electrochemical cells (LECs) have become a very interesting area of development in what is now the widely studied field of "organic electroluminescence" [1-3]. Although still lacking the life-time performances required for use in displays, they are nevertheless important as their performances are constantly improving.

The simulation of LECs has not received much attention, probably because the practical applications of LECs are still rather limited [4-8]. In an effort to achieve a better understanding of these devices, the model used previously [9] to describe the behaviour of Ru(bpy)₃²⁺-based LECs is modified to include ionic equilibrium effects. Previous data suggested that the residual solvent may play an important role in the behaviour of LECs [9, 10], while recent experimental data [11, 12] prove that the water content is critical for device behaviour, and devices with very low water content behave more like light-emitting diodes rather than LECs. Moreover, recent experimental data confirm that ionic equilibrium is quite important for device operation [13, 14]. Therefore, the "weak electrolyte" assumption, and consequently the effect of dynamic electrolyte dissociation during operation, should be considered in order to be able to better understand the behaviour of these devices and may help to make qualitative predictions.

Model description and simulation parameters

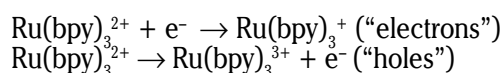
The main features of the model proposed for describing the behaviour of Ru(bpy)₃²⁺-type "solid-state" LECs are described below (see also [9]):

Assumptions and approximations

- Gouy-Chapman-Stern model for describing the interfaces near each electrode;
- the movement of charge carriers are described by the Nernst-Planck equations;
- the film is a continuous medium, without taking into account the size of the ions;
- mobilities and diffusion coefficients are related through the Einstein equation;
- the (local) concentrations of inert ions are related to each other through the ionic equilibrium condition;
- mobilities of "electrons" and "holes" are field independent;

- activity coefficients are considered to be constant throughout the film at all times.

- The reactions taking place at the electrodes:



- Individual charge injection potential barriers for "electrons" and "holes", at the cathode and anode, respectively (see the reactions above) are given by ($0 < \nu < 1$; for $\nu = 0.5$ the potential barriers are identical):

$$V_c^0 = \nu \times V_b; V_a^0 = (1 - \nu) \times V_b$$

where V_b is the "band-gap" of the emitting material, V_c^0 and V_a^0 being used in eq. (7). Such an approach allows for asymmetrical charge injection of, say, electrons compared to holes (see [9] for more details and [1, 15]). The "band-gap" can be estimated roughly either from cyclic voltammetry experiments or from the wavelength of the emitted light [29].

Model equations

- Flux equations for each mobile species:

$$J_i(x,t) = -D_i \left(\frac{\partial C_i(x,t)}{\partial x} - z_i C_i(x,t) \frac{F}{RT} E(x,t) \right), \quad i = p, n, X \quad (1)$$

- Continuity equations for ions:

$$\frac{\partial C_X(x,t)}{\partial t} = -\frac{\partial J_X(x,t)}{\partial x} \quad (2)$$

$$\frac{\partial C_C(x,t)}{\partial t} = 0 \quad (3)$$

for anions (X, mobile) and cations (C, fixed). Note that these are valid only for constant mobile anion concentrations. If an association-dissociation of ions (and ion-pairs) equilibrium is involved, eqs. (2) and (3) should be replaced by eqs (2') and (3') below.

- Continuity equations for "electrons" (n) and "holes" (p):

$$\frac{\partial C_i(x,t)}{\partial t} = -\frac{\partial J_i(x,t)}{\partial x} - k \times C_p C_n \quad (4)$$

* email: mihai@cedra.chfiz.pub.ro; Tel: 0727753961

with $i = n, p$.

- Poisson equation

$$\frac{\partial E(x,t)}{\partial x} = \frac{1}{\varepsilon} \sum_i z_i C_i(x,t), \quad i = n, p, X, C; \quad \frac{\partial \Phi(x,t)}{\partial x} = -E(x,t) \quad (5)$$

The letters p, n, X and C refer to "holes" (Ru^{III} sites), "electrons" (Ru^{I} sites), mobile anions and fixed cations, respectively. $J_i(x,t)$, $C_i(x,t)$, D_i and z_i are the fluxes, concentrations, diffusion coefficients and charges of species i , k is the electron-hole recombination rate constant, $\Phi(x,t)$ is the electric potential and $E(x,t)$ is the electric field.

The current flowing through the film is given by:

$$I = F \sum_{i=p,n,X} z_i J_i(x,t) + \varepsilon \varepsilon_0 \frac{\partial E(x,t)}{\partial t} \quad (6)$$

where the second term represents the Maxwell's displacement current with ε and ε_0 being the relative dielectric constant and vacuum permittivity respectively (similar to a capacitive current).

In addition to these equations, the boundary and initial conditions must be defined as following (the boundary conditions are given only for the cathode, $x = 0$; similar relationships can be written for the anode, $x = 1$, too):

- The Nernst equation for "electrons" and "holes" at each electrode:

$$\begin{aligned} \Phi_c - \Phi_c^0 &= V_c^0 + \frac{RT}{F} \ln \left(\frac{C^* - C_n(0,t) - C_p(0,t)}{C_n(0,t)} \right) = \\ &= V_a^0 + \frac{RT}{F} \ln \left(\frac{C_p(0,t)}{C^* - C_n(0,t) - C_p(0,t)} \right) \end{aligned} \quad (7)$$

where Φ_c is the applied electric potential at the cathode contact and Φ_c^0 is the electric potential at the Stern layer (within the Stern layer the drop from Φ_c to Φ_c^0 is assumed to be linear). C^* is the total concentration of the "solid" $\text{Ru}(\text{bpy})_3(\text{ClO}_4)_2$, estimated from crystal data [9].

- Blocking electrode conditions for mobile anions;

$$\left(\frac{\partial C_x(x,t)}{\partial x} \right)_{x=0} - C_x(0,t) \frac{F}{RT} \left(\frac{\partial \Phi(x,t)}{\partial x} \right)_{x=0} = 0 \quad (8)$$

For the fixed cations the concentration C_c at any given grid point can be calculated from eq. (3') as a function of the concentration of anions, C_x . Alternatively, if the concentration of mobile anions is considered fixed, then C_c is constant throughout the film at all times.

- Electric field continuity at the boundary between the Stern compact layer (inside which the electric field is assumed to be constant) and the rest of the film:

$$\left(\frac{\partial \Phi}{\partial x} \right)_{x=0} = \frac{\Phi_c - \Phi_c^0}{d} \quad (9)$$

where d is the thickness of the Stern (compact) layer.

- The electric potential at each electrode is taken as one half the applied voltage:

$$-\Phi_c = \Phi_a = V_{\text{app}}/2 \quad (10)$$

where V_{app} is the applied voltage.

- Initially (at zero-bias) the concentrations of ions are considered constant throughout the film (and calculated

using the value for the dissociation equilibrium constant, K) and the concentrations of "electrons" and "holes" are considered to be zero.

- Taking into account the Wien effect means that the dissociation equilibrium constant, K , depends on the electric field [17, 18]:

$$\frac{K(E)}{K(0)} = \frac{I_1(4\sqrt{-\beta q})}{2\sqrt{-\beta q}} \quad (11)$$

where E is the electric field intensity, $K(0)$ is the dissociation equilibrium constant for zero electric field, I_1 is the first order modified Bessel function, q is the Bjerrum parameter and β is a parameter which depends on the electric field. For single-charge uni-univalent electrolytes, eq. (11) can be re-written as:

$$\frac{K(E)}{K(0)} = \frac{I_1 \left(2\sqrt{2q \frac{e}{kT}} |E| \right)}{\sqrt{2q \frac{e}{kT}} |E|} \quad (11')$$

where $|E|$ is the modulus of the electric field intensity and

$q = \frac{1}{4\pi 2\varepsilon\varepsilon_0 kT} \frac{e^2}{kT}$ is the Bjerrum length, ε being the relative dielectric constant. Thus K is no longer uniform throughout the film, but instead it depends on the electric field distribution.

Solving the equations:

The model equations (1) – (5) together with the boundary conditions are made spatially discrete using a non-uniform grid, with increasing number of points near each electrode, where the electric field is very large (see [9] for more details on computational procedures). Since the system of equations is very stiff, the Scharfetter-Gummel method (which assumes constant fluxes in each discrete box) was chosen as a spatial discretization scheme [19], allowing for much better accuracy in regions with large electric fields. For the time discretization, a fully implicit Euler scheme was chosen.

The discrete system of algebraic equations is then solved by the Newton-Raphson method, taking advantage of the block 4 x 4 tridiagonal Jacobian's matrix (all simulations were performed using an analytical Jacobian). The Newton-Raphson iterations were stopped when the difference between two successive values for all (dimensionless) concentrations at all grid points was less than 10^{-5} . The accuracy of the simulated data was further checked using eq. (6), which must yield a spatially independent current. If the current is not constant (to a certain degree of accuracy) throughout the device, then the accuracy of the simulation must be increased, either by increasing the number of grid points, or decreasing the tolerance for the Newton-Raphson iterations (or both). For high accuracy, the simulations presented here were performed using a total of 440 grid points: 100 points near each electrode (where the electric field is very large) and 240 points in the bulk of the device (where the electric field is relatively low). A 0.1% maximum error in current along the device was considered acceptable (for most cases the actual error was $\sim 0.05\%$ or even less).

For the simulations ran taking into account the Wien effect, the Bessel function was approximated using a classical series expansion [20].

The output values from the simulation give the concentration profiles for ions, "electrons" and "holes", the electric current and the potential distribution (or the

electric field) through the cell.

Typical running times for a current-time curve (at constant applied voltage) taken on a 3.2 GHz Pentium computer running Windows XP range from ~150 s for large values of K (when the steady state is attained fast) to about 300 s for low values of K (when the steady state is attained much slower). More details about the simulation procedure can be found in the supporting information of reference [9].

Main parameters used for simulation

For the simulations presented here, the following parameters were used [9]:

“Band-gap”: $V_b = 2.65$ V

Ratio between “electron” diffusion coefficient and anion diffusion coefficient: 500.

Ratio between “hole” diffusion coefficient and anion diffusion coefficient: 500.

$v = 0.35$.

$C^* = 1.8$ mole/L.

Compact layer thickness, $d = 0.85$ nm

Ionic dissociation equilibrium constant, $K = 5 \times 10^7$ mole/L, unless otherwise noted. Although the equilibrium constant is generally considered dimensionless, we choose to give units to K to stress that the value was not made dimensionless to ease the implementation of the numerical algorithm.

Applied voltage between the two contacts ranging from 2.1 to 2.8 V, unless otherwise noted.

Since for most parameters it is difficult to give even approximate values, all results are presented in dimensionless form:

- dimensionless current: $i = I \times L / FADC_0$, where I is the current (in A), A is the contact area (in cm^2), D is the diffusion coefficient of mobile anions (in cm^2/s), C_0 is the initial (zero-bias) free mobile anion concentration (in mole/ cm^3) and L is the cell thickness (in cm). In some cases the “corrected” current is used, i.e. the product between the dimensionless current and C_0 , $i \times C_0$, as it allows a better comparison for different values of K.

- dimensionless time: $\tau = Dt/L^2$, where D is the diffusion coefficient of mobile anions (in cm^2/s), t is the time (in seconds) and L is the device thickness (in cm).

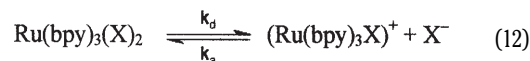
- dimensionless electric field: $f = LF/RT \times E$, where L is the device thickness (in cm) F is the Faraday constant, E is the electric field (V/cm) R is the gas constant and T is the absolute temperature.

In the previously used model [9] it was assumed that the *total* ionic concentration remains constant throughout the cell at all times. This means that the *total* number of ions during operation is exactly the same as for the unbiased device: the ions only re-arrange under bias. However this assumption, while somewhat simplifying the mathematical treatment, is physically unrealistic. If an ionic dissociation equilibrium is actually involved, this means that, locally, more ions can be generated and consequently the total number of ions should *increase* under bias compared to the zero-bias device. Therefore, even when there are relatively few ions to start with (low dissociation equilibrium constant), “electrons” and “holes” could still be injected at high enough concentrations, provided that the bias is large enough and maintained for a long enough time.

To describe the ionic equilibrium we shall assume for simplicity that the $\text{Ru}(\text{bpy})_3\text{X}_2$ compound (where X^- stands for the chemically inert anion, such as ClO_4^-) dissociates into $(\text{Ru}(\text{bpy})_3\text{X})^+$ and X^- only. The assumption may be

regarded as reasonable, as it would be difficult in a medium with very low water (or solvent) content to have a doubly charged cation, such as $\text{Ru}(\text{bpy})_3^{2+}$. Of course, introducing a second dissociation stage would not complicate the problem significantly, but it is felt that it would not bring out important conclusions, while the introduction of a second adjustable parameter (the second dissociation constant) complicates rather unnecessarily the interpretation of the simulation results.

Therefore, for the reasons detailed above, one may be confined to the following ionic equilibrium only:



which is established dynamically, i.e., it is characterized by one forward and one backward rate constants (k_d and k_a – the dissociation and association rate constants, respectively), related to each other through an equilibrium constant:

$$K = k_d/k_a = C_0^2/(C^* - C_0) \quad (13)$$

where $C_0 = C_{c0} = C_{x0}$ (the index “C” denotes the $\text{Ru}(\text{bpy})_3\text{X}^+$ cation and the index “X” represents the anion) is the initial (zero-bias) free anion concentration and C^* is the total concentration of ions, which can be estimated roughly from crystal data. We shall assume again that only the anions are mobile, as the $(\text{Ru}(\text{bpy})_3\text{X})^+$ ions are quite bulky, so we can express the local concentration of $\text{Ru}(\text{bpy})_3(\text{X})_2$ ion pairs through a balance between the anion concentration (C_x) and the total concentration of $\text{Ru}(\text{bpy})_3(\text{X})_2$ (C^*). The only difference from the previous model will be in the equations describing the ion movement; we can thus write for both the anions and cations the following equations instead of eqs. (2) and (3):

$$\frac{\partial C_x(x,t)}{\partial t} = -\frac{\partial J_x(x,t)}{\partial x} + k_d(C^* - C_c(x,t)) - k_a C_x(x,t) C_c(x,t)$$

$$\frac{\partial C_c(x,t)}{\partial t} = 0 + k_d(C^* - C_c(x,t)) - k_a C_x(x,t) C_c(x,t)$$

where J_x is the flux of anions (containing both the diffusion and migration terms). There is no such flux for cations, as they are immobile, but their concentration is no longer constant throughout the device, because of the combined effects of the anion movement and the ionic dissociation equilibrium.

By taking into account the ionic equilibrium, one introduces two more adjustable parameters: either one rate constant (say, k_d) and the equilibrium constant (K), or two rate constants (k_d and k_a). It turns out though that for most cases of practical interest only the equilibrium constant is important, as long as the dissociation/association processes are assumed to be very fast (essentially at equilibrium). Therefore, as long as both k_d and k_a are large enough – (for aqueous solutions, k_d is of the order of 10^7 s^{-1} ; see e.g. [21]) – their influence is reflected only in their ratio, as the ionic dissociation equilibrium constant K. It is conceivable that for “solid-state” media, as the LECs are considered to be, k_d and k_a are significantly smaller than the corresponding values for liquids, but even if they are four or five orders of magnitude smaller, the dissociation/association processes can still be considered very fast (essentially at equilibrium) on the time scale of the simulations.

By changing the value of K, one may describe the possible effects that the water/solvent content has on the behaviour of LECs.

Experimental part

The experimental data are taken from reference [9] and refer to films of $\text{Ru}(\text{bpy})_3(\text{ClO}_4)_2$ of about 100 nm thickness spin-coated onto ITO, with the top contact made with Ga-In liquid alloy and operated under ambient conditions at room temperature ($\sim 20^\circ\text{C}$). The applied voltage between contacts is either constant, ranging from 2.1 to 2.5 V (e.g. fig. 5), or continuously scanned starting from 0V with 25 mV/s (fig. 6 – as the currents below ~ 1.2 V are quite small and noisy, only the part above this arbitrary chosen threshold value is shown).

Results and discussions

There are several relevant features that result from device simulation taking into account the ionic equilibrium, discussed below.

The ionic equilibrium explains better device behaviour as the water content lowers; in fact, the constant ionic concentration is unrealistic in this case.

When the ionic equilibrium is established at any given time, it means that every time an anion moves, more ions will be created locally because of the ionic equilibrium. Even starting with a very low free ionic concentration at zero bias, if one waits long enough (ion movement is quite slow), a significant amount of ions can be generated to inject significant charge at the electrodes through an electrochemical mechanism. The smaller the initial free ionic concentration, the longer one has to wait until steady-state current is reached. One can picture the whole process in a naive manner: every movement of ions creates locally more ions; these “new” ions will move too, their movement creating more ions, etc., until a steady-state is reached. The main difference from the previous model is that now the steady-state is reached much slower (depending, of course, on the initial concentration of free ions, figs. 1 and 2).

The time needed to reach steady-state increases significantly as the dissociation equilibrium constant decreases (fig. 2). This slow time reflects not only the intrinsically slow diffusion coefficient of the chemically inert mobile ions, but also the dynamic equilibrium and mobile ion “generation” under bias. Several experimental studies have described LEC-type devices with very long response times [22-24], suggesting that ionic equilibrium may be important in LECs. Also, adding an ionic liquid to an LEC device, favouring both the ionic dissociation and ion movement, leads to a dramatic decrease (of about an order of magnitude) in turn-on times for such devices [25].

The total number of ions under bias at steady-state is *not* the same for different applied voltages, and increases with applied voltage (fig. 3 and table 1). As the voltage increases, due to the build-up of a space charge near the electrodes, more free ions will be generated as the ionic dissociation equilibrium in reaction (12) will be shifted to the right. Also, the concentration of cations will no longer be constant throughout the device, even if they are considered to be fixed: the movement of mobile anions shifts the equilibrium in reaction (12) either towards the formation of more cations (near the cathode, where the concentration of anions is very small) or towards the formation of ion-pairs (near the anode, where the concentration of anions is very large, fig. 3 and 4). This behaviour can explain why even for quite low initial (zero-bias) mobile ion concentration, a device may still exhibit LEC behaviour if one waits long enough for the ions to be generated under bias.

The simulation results show a fair agreement with

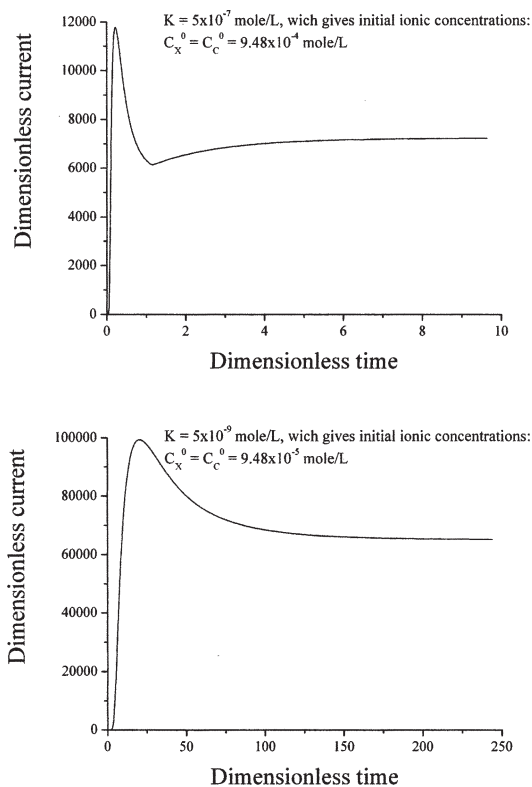


Fig. 1. Comparison between the dimensionless current transients at 2.5 V for two values of the ionic dissociation equilibrium constants K

Table 1

TOTAL NUMBER OF CATIONS IN THE DEVICE FOR $K = 5 \times 10^{-7}$ MOLE/L AT VARIOUS VOLTAGES. THE NUMBER OF CATIONS IS OBTAINED BY INTEGRATING THE (DIMENSIONLESS) CONCENTRATION PROFILES OF CATIONS (FIG. 3) OVER THE ENTIRE (DIMENSIONLESS) THICKNESS OF THE FILM AND ASSUMING UNIT AREA FOR THE CONTACTS. NOTE THAT AT ZERO-BIAS THE TOTAL NUMBER OF CATIONS IS EQUAL TO 1.0.

Voltage (V)	N_c^*
2.0	4.273
2.2	4.888
2.4	5.545
2.6	8.328
2.8	15.972

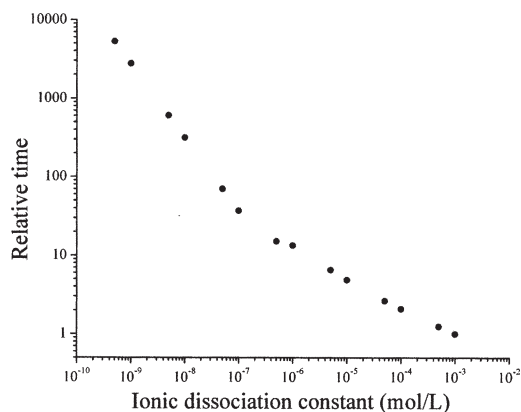


Fig. 2. Dependence of the relative time needed to reach 90% of the steady-state current with the ionic dissociation equilibrium value at 2.5 V. All values are relative to the (dimensionless) time obtained for $K = 10^{-3}$ mol/L, which is taken as unity.

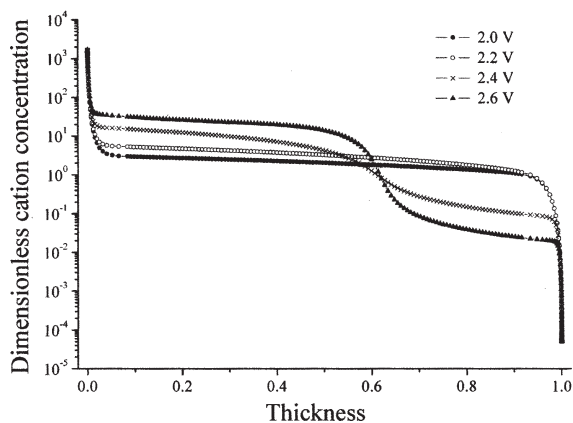


Fig. 3. Steady-state dimensionless cation concentration (C_c) throughout the film at various bias voltages for $K = 5 \times 10^{-7}$ mol/L. The zero-bias dimensionless concentration of cations is 1 for all cases.

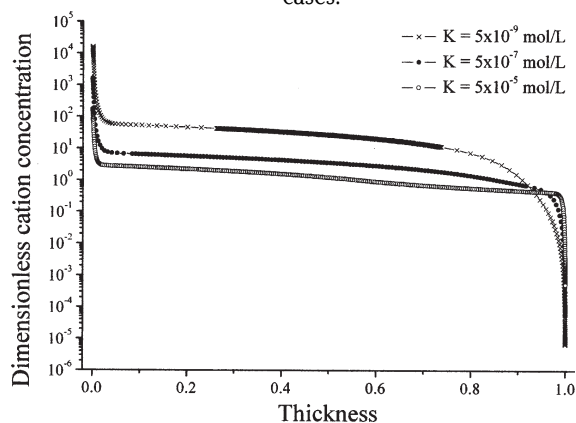


Fig. 4. Steady-state dimensionless cation concentration (C_c) throughout the film at 2.5 V for three values of the dissociation equilibrium constant. The zero-bias dimensionless concentration of cations is 1 for all cases.

experimental data, especially when lower initial free ionic concentrations are used (fig. 5, 6). Quantitative overlap between the simulated and experimental data is however beyond the purpose of this paper: there are too many unknowns which can either be more or less freely adjusted (such as the ionic dissociation equilibrium constant, diffusion coefficients for all species, solvent/water content of the films, etc.) or else not yet taken into account (such as a mechanism for device degradation, related to the residual solvent present in the device), rendering a quantitative approach a rather fruitless task for the present time.

The ionic equilibrium may be related to the concentration of residual solvent which may be present in the film. Experimental data [9, 11, 12] show that devices prepared and operated under various conditions have quite different response times, and that the concentration of residual solvent is very important. The simulations show that the steady-state current decreases as the ionic equilibrium constant decreases (fig. 7), but below a value of $K \sim 5 \times 10^{-7}$ mol/L the “corrected” current remains almost constant.

It was assumed however that the ratios for “electron”/anion and “hole”/anion diffusion coefficients do not change with K , which is quite unrealistic: if the decrease in K is associated with a lowering in water/solvent content, then it is quite likely that all diffusion coefficients (for anion, “electron” and “holes”) decrease as the solvent content decreases. For example, it has been reported that the electron self-exchange rate constant decreases by roughly

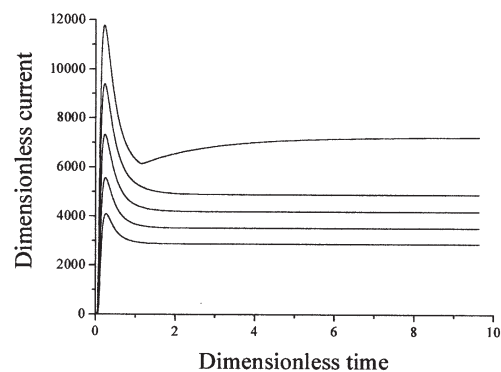
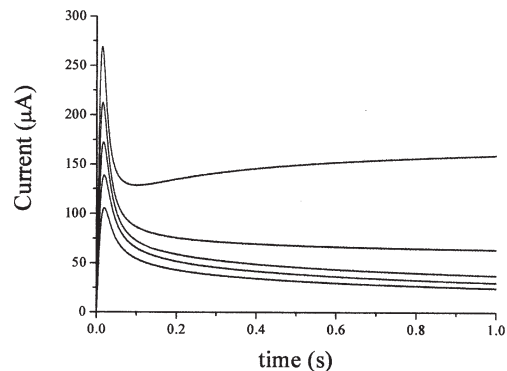


Fig. 5. Comparison between experimental (top) and simulated (bottom) current transients. The bias voltage increases from bottom to top from 2.1 to 2.5 V in 0.1 V steps. The experimental curves are reproduced with permission from figure 4 in ref. [9], copyright 2002 American Chemical Society.

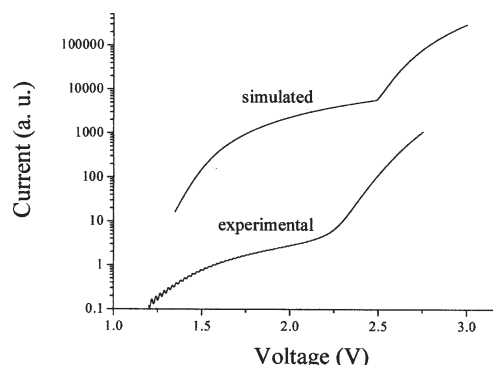


Fig. 6. Comparison between the simulated and experimental current-voltage curves (both at 25 mVs^{-1}). The relative current for the simulated curve has been purposely shifted upwards to allow for a better comparison of the curves’ shapes. The experimental curve is reproduced with permission from Figure 7 in ref. [9], copyright 2002 American Chemical Society.

an order of magnitude going from solvent-wetted to “dry” vinyl-bipyridine-based Os polymers [26]. The electron self-exchange rate constant is linked to the electron-hopping diffusion coefficient (e.g. [27]), and therefore to the “electron” and “hole” diffusion coefficients. It is thus conceivable that *both* ion and electron movements are affected by the lower solvent content, but it is difficult to evaluate this influence in LEC-type devices. Studies on the same vinyl-bipyridine-based Os polymers show that when comparing “dry” and solvent-wetted films the diffusion coefficient of ions drops by a factor of 10^4 , while the electron diffusion coefficient drops by a factor of only 10 [28]; however, it is not clear how “dry” such films are. For a $\text{Ru}(\text{bpy})_3$ -type LEC (without purposely added solvent), it is very difficult to remove the last traces of solvent and water, while at the same time it is also difficult to evaluate how

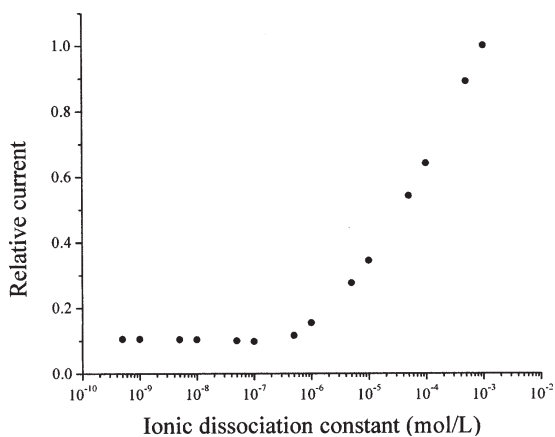


Fig. 7. Dependence of the relative current with the ionic dissociation equilibrium K at 2.5 V. All values are relative to the (dimensionless) current for $K = 10^{-3}$ mole/L, which is taken as unity and corrected for the change in the zero-bias concentration as K changes.

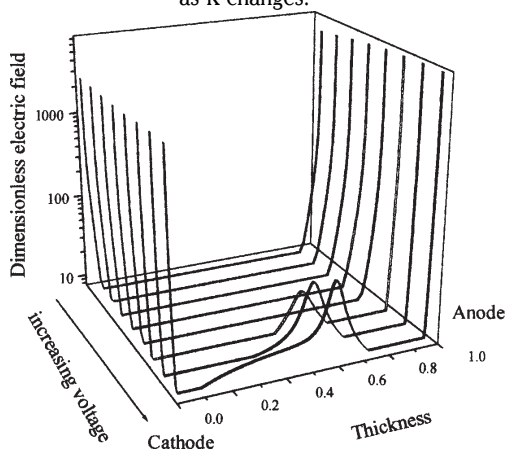


Fig. 8. Simulated steady state electric fields. While at lower biases the bulk of the device is essentially electroneutral, the electric field builds up at larger biases in the recombination region. The curves are simulated for bias voltages from 2.1 V to 2.8 V in 0.1 V steps.

much residual water (or solvent) is present in the device, even when prepared under inert conditions [10, 12].

Therefore, the plateau in figure 7 for low ionic dissociation constants should be regarded only as an apparent one: it does not mean that the effective current does not decrease as the ionic dissociation constant lowers, but rather that it is proportional to the concentration of ions at zero-bias (see the definition of the “corrected current”). As mentioned above, the experiments do show that the steady-state current decreases by several orders of magnitude and the response times become longer when the water content is lowered [12] (which in turn should lead to a lower value of the ionic dissociation constant), suggesting that ionic equilibrium may be important. Also, ref. [11] shows that increasing the humidity of the environment in which an LEC is operated leads to a large decrease in the response time and increase in current (both by about an order of magnitude from 0% to 63% humidity). Care must be taken though when comparing simulated data to experimental ones, since for slow response-time devices any voltage sweep experiment performed using reasonable sweep-rates (spanning from about 0.5 mVs^{-1} to 50 mVs^{-1}) is bound to be a non-steady-state one. In fact, for very low ionic dissociation constants (such as for the “very dry” devices in ref. [12]) it is likely that the ion movement is hindered to such an extent that there are no longer mobile ions present. In this case the charge injection

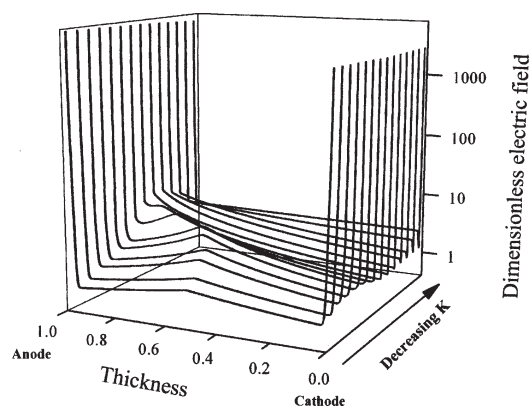


Fig. 9. Simulated electric field at 2.5 V applied bias for various values of the ionic dissociation constant.

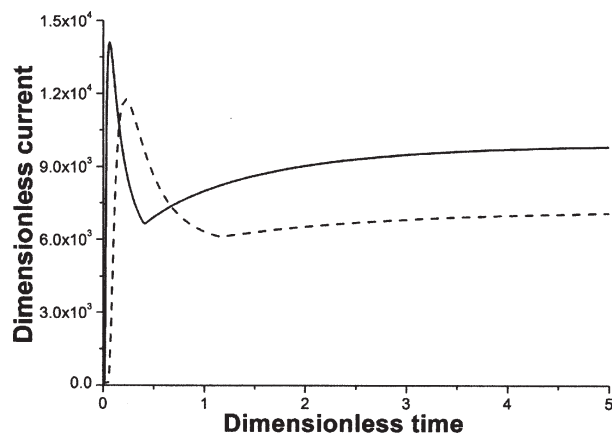


Fig. 10. Comparison between the current transients at 2.5 V for $K = 5 \cdot 10^{-7}$ mole/L with (solid line) and without (dashed line) Wien effect.

at the electrodes is probably no longer achieved by an electrochemical mechanism, but rather becomes contact-dependent, and the device, instead of an LEC, becomes a typical organic light-emitting diode [29]. It is also worth noting that charge-neutral Ru(II) emitters show a typical “diode-like” behaviour, since no free ions are expected in such materials [30].

As expected for an electrochemical charge injection mechanism, the electric field builds up near the electrodes, with the bulk of the device being essentially electroneutral for not too large biases (fig. 8). Only at larger biases, where significant “electron” and “hole” concentrations are built, the bulk electric field reaches significant values, and the cell may no longer be thought to be electroneutral. For the same applied bias (relatively low), the change in the steady-state electric field profile does not change much as the dissociation equilibrium is varied (fig. 9). Of course, the time needed to reach the steady-state increases significantly as the dissociation constant decreases.

Taking into account the second Wien effect: the model is further refined by including the high field weak-electrolyte dissociation effect, or “the second Wien effect” [17]. The second Wien effect shows that under an intense electric field the dissociation constant of a (weak) electrolyte increases and it has been suggested that it may influence the electric conductivity of conducting polymers [31]. As a consequence, in LEC-type devices near the electrodes (where the electric field is very large) the ion-pairs will eventually dissociate more, leading to an increase in the concentration of mobile ions. The main influence of the Wien effect in such devices, as a result of better dissociation in the regions with high electric field near the electrodes, is an increased ionic conductivity. As a result, the transients

become slightly faster, as expected, since in fact the Wien effect leads to a slightly larger dissociation constant, exactly where this dissociation is important, namely near the electrodes where the electric field is large.

Conclusions

The ionic dissociation equilibrium provides a more complete, albeit qualitative, picture of LECs and their behaviour, helping to a better understanding of these devices. The assumption of constant mobile ion concentration is replaced by a more physically realistic condition, which involves the dynamical equilibrium between free ions and ion-pairs. It is shown that for low ionic dissociation equilibrium constants, which may be related to the concentration of residual solvent present in the film, the time-response becomes very long. Thus, the slow response times for LECs may in fact be due to two factors: very low dissociation equilibrium constant (that is, very low free ion concentration at zero-bias) and very slow ion movement. It is also likely that when the concentration of residual solvent (which is linked to the concentration of mobile ions) becomes very low, the device no longer behaves as an electrochemical cell.

Acknowledgements: Support from CNCSIS (grant no. 277/2005) is acknowledged. Nicoleta Dobre is grateful to University "POLITEHNICA" Bucharest for financial support through project DoctInvest (ID 76813). The authors wish to thank prof. Allen J. Bard and dr. Donald Pile for fruitful discussions.

References

1. ZHEN C., CHUAI Y., LAO C., HUANG L., ZOU D., LEE D.N., KIM B.H., *Appl. Phys. Lett.*, **87**, 2005, p. 093508.
2. HOLDER E., LANGEVELD B.M.W., SCHUBERT U.S., *Adv. Mater.*, **17**, 2005, p. 1109.
3. COE B.J., CURATI N.R.M., *Comments Inorg. Chem.*, **25**, 2004, p. 147.
4. deMELLO J.C., TESSLER N., GRAHAM S.C., FRIEND R.H. *Phys. Rev. B* **57**, 1998, p. 12951.
5. deMELLO J.C., *J. Comput. Phys.*, **181**, 2002, p. 564.
6. deMELLO J.C., *Phys. Rev. B*, **66**, 2002, p. 235210.
7. CHENG C.H.W., LIN F., LONERGAN M.C. *J. Phys. Chem. B*, **109**, 2005, p. 10168.

8. MILLS T.J., LONERGAN M.C., *Phys Rev B*, **85**, 2012, p. 035203.
9. BUDA M., KALYUZHNY G., BARD A.J. *J. Am. Chem. Soc.*, **124**, 2002, p. 6090.
10. KALYUZHNY G., BUDA M., MCNEILL J., BARBARA P., BARD A.J., *J. Am. Chem. Soc.*, **125**, 2003, p. 6272.
11. PILE D.L., BARD A.J., *Chem. Mater.*, **17**, 2005, p. 4212.
12. ZHAO W, LIU C.-Y., WANG Q.I., WHITE J.M., BARD A.J., *Chem. Mater.* **17**, 2005, p. 6403.
13. VAN REENEN S., JANSSEN R.A.J., KEMERINK M., *Adv. Funct. Mater.*, **22**, 2012, p. 4547.
14. ZHU Y., MA Y., ZHU J., *J. Lumin.*, **137**, 2013 p. 198.
15. DINI D., *Chem. Mater.* **17**, 2005, p. 1933.
16. UNGUREANU E.-M., BUICA, G.-O., RAZUS A.C., BIRZAN L., WEISZ R., BUJDUVEANU M.-R., *Rev. Chim.*, **63**, 2012, p. 27.
17. ONSAGER L. *J. Phys. Chem.*, **2**, 1934, p. 599.
18. MASON D.P., MCILROY D.K. *Physica A* **82**, 1975, p. 463.
19. SCHARFETTER D.L., GUMMEL H.K. *IEEE Trans. Electron Devices*, ED-16, 1969, p. 64.
20. ABRAMOWITZ M., STEGUN I.A., (editors) *Handbook of Mathematical Functions*, (Washington: National Bureau of Standards; reprinted 1972, Dover Publications, New York), p. 382.
21. BUCHNER R., BARTEL J., *J. Mol. Liquids*, **63**, 1995, p. 55.
22. EDMAN L., MOSES D., HEEGER A.J., *Synth. Met.*, **138**, 2003, p. 441.
23. BOLINK H.J., CAPELLI L., CORONADO E., GRÄTZEL M., NAZEERUDDIN M.K., *J. Am. Chem. Soc.*, **128**, 2006, p. 46.
24. BOLINK H.J., CAPELLI L., CORONADO E., GAVI A P., *Inorg. Chem.*, **44**, 2005, p. 5966.
25. PARKER S.T., SLINKER J.D., LOWRY M.S., COX M.P., BERNHARD S., MALLIARAS G.G., *Chem. Mater.* **17**, 2005, p. 3187.
26. SURRIDGE N.A., ZVANUT M.E., KEENE F.R., SOSNOFF C.S., SILVER M., MURRAY R.W., *J. Phys. Chem.*, **96**, 1992, p. 962.
27. TERRILL R.H., MURRAY R.W., *Mol. Electron.* 1997, 215.
28. SURRIDGE N.A., JERNIGAN J.C., DALTON E.F., BUCK R.P., WATANABE M., ZHANG H., PINKERTON M., WOOSTER T.T., LONGMIRE M.L., FACCI J.S., MURRAY R.W., *Faraday Discuss.*, **88**, 1989, p. 1.
29. BUDA M., Chapter 10: ECL polymers and devices, in Bard AJ (ed) *Electrogenerated chemiluminescence*. Marcel Dekker, New York, 2004, p. 499-503.
30. TUNG Y.L., LEE S.W., CHI Y., CHEN L.S., SHU C.F., WU F., CARTY A.J., CHOU P.T., PENG S.M., LEE G.H., *Adv. Mater.* **17**, 2005, 1059.
31. RIBÓ, J.M., ANGLADA M.C., HERNANDEZ J.M., ZHANG X., FERRER-ANGLADA N., CHAIBI A., MOVAGHAR B., *Synth. Met.*, **97**, 1998, 229.

Manuscript received: 17.06.2013